Available online at www.sciencedirect.com
SCIENCE DIRECT®
Journal of Sound and Vibration 276 (2004) 13–26
JOURNAL OF SOUND AND VIBRATION
www.elsevier.com/locate/jsvi

Sound speed criterion for two-phase critical flow

M.-S. Chung*, S.-B. Park, H.-K. Lee

Agency for Defense Development, 2nd R&D Center, P.O. Box 18, Chinhae, Kyungnam 645-600, South Korea

Received 17 June 2002; accepted 14 July 2003

Abstract

Critical flow simulation for non-homogeneous, non-equilibrium two-phase flows is improved by applying a new sound speed model which is derived from the characteristic analysis of hyperbolic two-fluid model. The hyperbolicity of two-fluid model was based on the concept of surface tension for the interfacial pressure jump terms in the momentum equations. Real eigenvalues obtained as the closed-form solution of characteristic polynomial represent the sound speeds in the bubbly flow regime that agree well with the existing experimental data. The analytic sound speed is consistent with that obtained by the earlier study of Nguyen et al. though there is a difference between them especially in the limiting condition. The present sound speed shows more reasonable result in that condition than Nguyen et al.'s does. The present critical flow criterion derived by the present sound speed is employed in the MARS code and is assessed by treating several nozzle flow tests. The assessment results, without any adjustment made by some discharge coefficients, demonstrate more accurate predictions of critical flow rate than those of the earlier critical flow calculations in the bubbly flow regime.

1. Introduction

Although the homogeneous equilibrium model is not a bad way of predicting the critical mass flow in long pipes, the non-homogeneous non-equilibrium critical flow model is a matter of great importance in the break of short pipes and the leakage of pressurized vessel where there is not sufficient time for equilibrium to be achieved and when the relative motion is not repressed by interfacial force.

The amount of two-phase fluid transportation rate through the pipe depends largely on the critical condition of two-phase mixture that is represented by mixture sound speed near the minimum cross-section because it provides system boundary conditions during flow transients.

*Corresponding author. Tel.: +82-55-540-6134.
E-mail address: s_clarinet@hotmail.com (M.-S. Chung).

0022-460X/$ - see front matter
doi:10.1016/j.jsv.2003.07.003

Engineering significance of the critical flow model led to a development of various empirical and mechanistic models, such as Moody [1], Henry–Fauske [2], Trapp–Ransom [3] models, and so on. However, accuracy of these models is still in question especially during thermal non-equilibrium conditions.

Critical flow condition is defined as the condition where mass discharge from a system becomes independent of conditions downstream, i.e., the condition where acoustic signals can no longer propagate upstream. This occurs when the fluid velocity equals or exceeds the propagation speed. Thus, it can be said that critical flow condition strongly relates with the mechanistic property of a fluid flow governed by the sound wave propagation characteristics, i.e., eigenvalues of the equation system.

The critical flow model of MARS [4] is based on Trapp–Ransom model [3]. The Trapp–Ransom model incorporated an analytic choking criterion for non-homogeneous, equilibrium two-phase flow. The two-fluid model for the conditions of thermal equilibrium is employed in the Trapp–Ransom model, which consists of overall mass conservation, two phasic momentum equations and the mixture entropy equation.

The momentum equations include the interface force terms called virtual mass terms representing relative acceleration: see Refs. [5,6]. Trapp and Ransom derived an analytic choking criterion that includes relative phasic acceleration terms and derivative-dependent mass transfer based on the characteristic analysis of this two-fluid model [3]. However, it should be noted that this criterion is derived based on the thermal equilibrium assumption, thus, may not be applicable when the thermal non-equilibrium effect dominates.

Characteristics of a two-fluid equation system can be represented by system eigenvalues. The real part of the system eigenvalues results the velocities of signal propagation along the corresponding characteristic path in the space–time plane and the imaginary part represents the rate of amplitude growth of the signal propagating along the respective path. In the Trapp–Ransom model, the analytic form of sound speed was obtained by the characteristic analysis of non-homogeneous, equilibrium conditions and it under-predicted the sound speed in comparison with the experimental data in the bubbly flow regime [3]. Furthermore, the existence of the non-zero imaginary part of the system eigenvalues may result in the non-physical, short wavelength instability [7–9].

A new promising approach to removing the complex eigenvalues was proposed by Lee et al. [8] and Chung et al. [9–11]. We introduced new terms, i.e., interfacial pressure jump terms based on the surface tension terms into the momentum equations. Although quantitative amount of these terms is relatively very small, they contribute to hyperbolicity of the equation system, even without the conventional virtual mass or artificial viscosity terms. And the eigenvalues obtained analytically represent comparable sound speed with the existing measured data as well as the analytic result produced by Nguyen et al. [12] for bubbly flow.

In this study, we propose a new critical flow criterion for the two-phase bubbly flow regime based on the hyperbolic two-fluid model. Then, new critical flow criterion is implemented in the MARS code and assessed using Marviken nozzle flow tests [13].

We introduce the interfacial pressure jump terms in Section 2. Following the characteristic analysis of the system matrix in Section 3, we discuss how the new sound speed criterion is implemented in Section 4. Finally, in Section 5, we discuss the assessment results of new criterion through several nozzle tests.

2. Hyperbolic two-fluid model

Trapp and Ransom [3] investigated the impact of the virtual mass coefficient on the sound speed. Even with the 'zero' virtual mass coefficient, Trapp–Ransom model under-predicted the sound speed for the bubbly flow at low void fraction range, $\alpha_g < 0.5$. To preclude problems associated with the selection of a virtual mass coefficient, we exclude the virtual mass terms in the characteristic analysis and we only include the interfacial pressure jump term as follows.

The conservation laws provide one-dimensional two-fluid mass, momentum, and energy equations based on the area-averaged phasic properties.

Continuity:

$$\frac{\partial(\alpha_k \rho_k)}{\partial t} + \frac{\partial(\alpha_k \rho_k v_k)}{\partial x} = \phi_{c,k}. \tag{1}$$

Momentum:

$$\frac{\partial(\alpha_k \rho_k v_k)}{\partial t} + \frac{\partial(\alpha_k \rho_k v_k^2)}{\partial x} + \alpha_k \frac{\partial p_k}{\partial x} + (p_k - p_i)\frac{\partial \alpha_k}{\partial x} = \phi_{m,k}. \tag{2}$$

Internal energy:

$$\frac{\partial(\alpha_k \rho_k u_k)}{\partial t} + \frac{\partial(\alpha_k \rho_k v_k u_k)}{\partial x} + p_k \frac{\partial \alpha_k}{\partial t} + p_k \frac{\partial(\alpha_k v_k)}{\partial x} = \phi_{e,k}. \tag{3}$$

The notation α_k, ρ_k, p_k, v_k, and u_k denote volume fraction, density, pressure, velocity, and internal energy, respectively, where phasic component $k = g$ is for the gas and $k = l$ is for the liquid. We use an additive equation, $\alpha_g + \alpha_l = 1$. The source terms like $\phi_{c,k}$, $\phi_{m,k}$, and $\phi_{e,k}$ depend on algebraic forms, therefore, they do not alter mathematical property of the above differential equation system.

The interfacial pressure jump term on the left hand side of momentum equation (2), $(p_k - p_i)\partial\alpha_k/\partial x$, is related with the surface tension as introduced in Refs. [8–11]. Its salient feature is not that the pressure has a jump at the interface but that its gradient is continuous across the interface for bubbles in equilibrium. Consequently, we obtain the interfacial pressure jump terms as

$$(p_g - p_i)\frac{\partial \alpha_g}{\partial x} = L_m\left(1 - \frac{R_g}{2}\frac{\partial a_i}{\partial \alpha_g}\right)\frac{\partial \alpha_g}{\partial x} = C_i L_m \frac{\partial \alpha_g}{\partial x}, \tag{4}$$

$$(p_i - p_l)\frac{\partial \alpha_l}{\partial x} = -L_m\left(1 + \frac{R_l}{2}\frac{\partial a_i}{\partial \alpha_l}\right)\frac{\partial \alpha_l}{\partial x} = -C_i L_m \frac{\partial \alpha_l}{\partial x}. \tag{5}$$

We use the interfacial area density relation for the bubbly flow, $a_i = 3.6\alpha_g/D$, suggested by Ishii and Mishima [14]. The averaged bubble diameter D is generally obtained by using the Weber number definition, $We \equiv 2D\rho_l(v_g - v_l)^2/\sigma$. However, if we simply assume that two radii R_g and R_l are equal to half of the averaged bubble diameter D, then the coefficient of interfacial pressure jump C_i becomes constant having an order of magnitude $O(10^{-1})$: see Ref. [10]. Since the fluid bulk modulus is $L_k \equiv \rho_k C_k^2$ and it holds that $L_g \ll L_l$, the mixture bulk modulus yields $L_m \approx L_g/\alpha_g$ as shown by Chung et al. [9,11]. We assume here that the order of magnitude of the mixture bulk modulus with constant is almost equal to that of the gas by taking $\alpha_g \approx O(10^{-1})$ for bubbly

flow, which gives then

$$C_i L_m = \rho_g C_g^2. \tag{6}$$

3. Sound speed for bubbly flow

The eigenvalues of the equation system represent the wave speed of small-amplitude short wavelength perturbations as Whitham [15] indicated. For long wavelength disturbances, dispersion and source terms play a more important role while, for large amplitude disturbances, the non-linear wave interaction is dominant. If the eigenvalues are all real, the initial value problem is well posed and stable against small disturbances.

In a matrix form, the mass, momentum, and internal energy equations become

$$\frac{\partial U}{\partial t} + G\frac{\partial U}{\partial x} = E. \tag{7}$$

The eigenvalues of matrix G in Eq. (7) are determined by a sixth order polynomial equation:

$$P_6(\lambda) = (\lambda - v_g)(\lambda - v_l)\left[\lambda^4 + K_1\lambda^3 + K_2\lambda^2 + K_3\lambda + K_4\right] = 0, \tag{8}$$

where the coefficients are expressed as functions of phasic properties:

$$K_1 = -2(v_g + v_l),$$

$$K_2 = (v_g + v_l)^2 + 2v_g v_l - (C_g^2 + C_l^2),$$

$$K_3 = 2\{v_g(C_l^2 - v_l^2) + v_l(C_g^2 - v_g^2)\},$$

$$K_4 = (C_l^2 - v_l^2)(C_g^2 - v_g^2).$$

The closed-form solution to the characteristic Eq. (8) gives a set of six real eigenvalues as listed in Table 1. The first two simple eigenvalues, λ_1 and λ_2, yield phasic convection velocities. Two eigenvalues, λ_3 and λ_5 with zero phasic velocities, i.e., $v_g = v_l = 0$, represent the sound speeds of the gas and the liquid phase, respectively. The total sound speed of bubbly flow can be expressed in the following form weighted by void fraction as

$$C_t = \frac{\lambda_3\lambda_5}{\alpha_l\lambda_3 + \alpha_g\lambda_5}. \tag{9}$$

By applying the closed-form solution of Eq. (8), we can get

$$C_t = \frac{C_g C_l\sqrt{\dfrac{\rho_g C_g^2}{\alpha_l\rho_g C_g^2 + \alpha_g\rho_l C_l^2}}}{\alpha_l C_g + \alpha_g C_l\sqrt{\dfrac{\rho_g C_g^2}{\alpha_l\rho_g C_g^2 + \alpha_g\rho_l C_l^2}}}. \tag{10}$$

For bubbly flow, the total sound speed agrees well with the experiment [16] in the void fraction range, $0 < \alpha_g < 0.3$, as shown in Fig. 1. As a limiting case, the sound speed becomes that of

Table 1
Eigenvalues of the two-fluid model

	Six eigenvalues
Bubbly flow regime	$\lambda_1 = v_g$ $\lambda_2 = v_l$ $\lambda_3 = v_g + C_g$ $\lambda_4 = v_g - C_g$ $\lambda_5 = v_l + C_l\sqrt{\dfrac{\rho_g C_g^2}{\alpha_l\rho_g C_g^2 + \alpha_g\rho_l C_l^2}}$ $\lambda_6 = v_l - C_l\sqrt{\dfrac{\rho_g C_g^2}{\alpha_l\rho_g C_g^2 + \alpha_g\rho_l C_l^2}}$

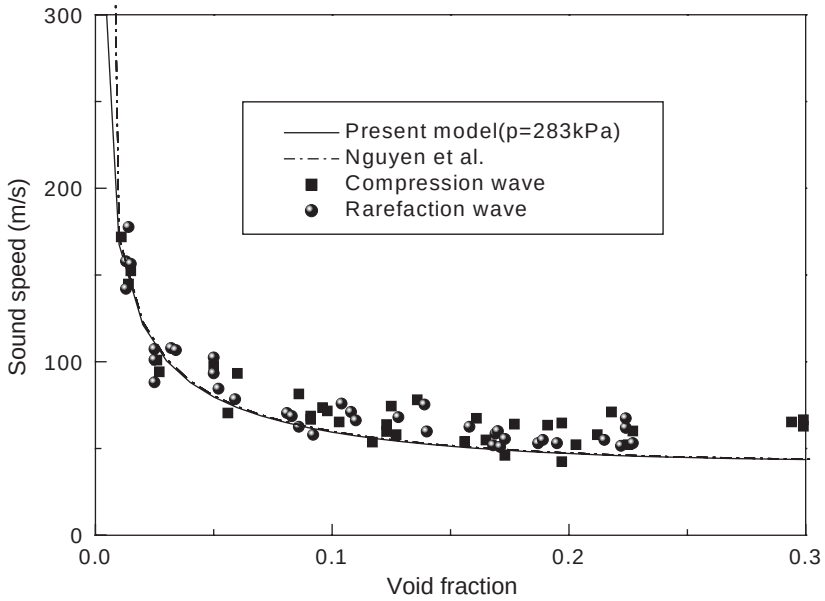

Fig. 1. Sound speed for vapor/water bubbly flow at $p = 283$ kPa.

a single-phase fluid when there is no bubble, i.e., $\alpha_g \to 0$. That is $\lim_{\alpha_g \to 0} C_t = C_l$, thus the result of two-phase flow is clearly reduced to that of single-phase in that condition.

Nguyen [12] also derived the sound speed from the equations of continuity and momentum, considering a stationary wave front in a moving single-phase medium as

$$C_t = \frac{C_g C_l \sqrt{\dfrac{\rho_g \rho_l}{\alpha_l \rho_g C_g^2 + \alpha_g \rho_l C_l^2}}}{\alpha_g \sqrt{\rho_g} + \alpha_l \sqrt{\rho_l}}. \tag{11}$$

Table 2
Comparison of the effective sound speed in each phase

Sound speed	Present model	Nguyen's model
Liquid phase	$C_l\sqrt{\frac{\rho_g C_g^2}{\alpha_l\rho_g C_g^2+\alpha_g\rho_l C_l^2}}$	$C_l\sqrt{\frac{\rho_g C_g^2}{\alpha_l\rho_g C_g^2+\alpha_g\rho_l C_l^2}}$
Gas phase	C_g	$C_g\sqrt{\frac{\rho_l C_l^2}{\alpha_l\rho_g C_g^2+\alpha_g\rho_l C_l^2}}$

He assumed that no phase change occurs during the propagation of sound wave and that the two-phase flow is confined by rigid wall. He also assumed that influence of the surface tension upon the pressure disturbance does not exist. Treating the interface of one phase as the elastic boundary of the other, a single-phase fluid surrounded by another fluid shows a dependency upon the bulk modulus of the other fluid, i.e. the sound speed decreases with an increasing elasticity of the other fluid.

However, Nguyen's model shows non-physical results that the sound speed of gas dispersed in liquid is much greater than that of single-phase gas at the limiting case $\alpha_g \to 0$, as shown in Table 2. For this reason, discrepancy between the present model and Nguyen's model in the range of extremely small void fraction, $\alpha_g < 0.02$, arises as shown in Fig. 1. An increasing deviation with experimental data shown in the void fraction range $\alpha_g > 0.3$ is possibly due to the flow regime transition effect.

We can find other useful experimental data at the condition of $p = 100$ kPa which are measured by Karplus [17] and Nakoryakov [18] and at the condition of $p = 117$ kPa measured by Hall [19] as shown in Figs. 2 and 3, respectively. At $p = 100$ kPa, the predicted sound speed for vapor/water bubbly flow well agrees with Ruggles' model [20]. Comparing with the experimental data [17,18], the predicted sound speed of the present, or the Ruggles' model [20] is under-predicted in the void fraction range, $0.05 < \alpha_g$. Further, the difference of sound speeds between the Ruggles' prediction and the experimental data become larger than that between the present model and the experimental data in the case of $0.1 < \alpha_g$. Fortunately, the calculated sound speeds are not far from the scatter of the experimental data [17,18]. However, at $p = 117$ kPa, the present sound speed of air/water bubbly flow shows excellent agreement with the Hall's data [19] as shown in Fig. 3.

4. Implementation of sound speed criterion

One subroutine contains the two-phase choking criterion used as a boundary condition for obtaining flow solutions in the MARS code. The MARS code is a multi-dimensional thermal hydraulic system code developed by KAERI. It is based on a two-fluid model calculated using the semi-implicit method [4] for transient analysis of integral systems. The implemented choking criterion imposes on the junctions determined to be in a choked state. If the choking is predicted, Eq. (12) is then written in terms of new-time phasic velocities and solved in conjunction with a

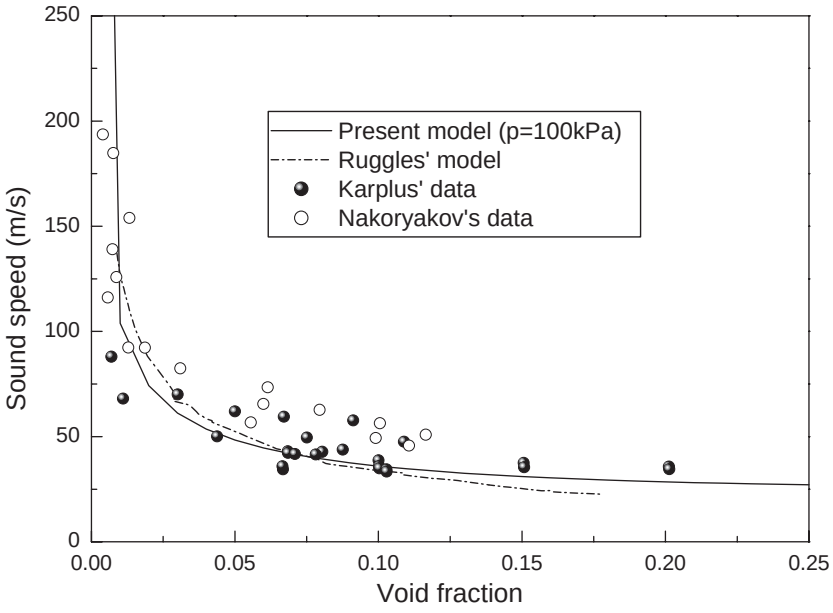

Fig. 2. Sound speed for vapor/water bubbly flow at $p = 100$ kPa.

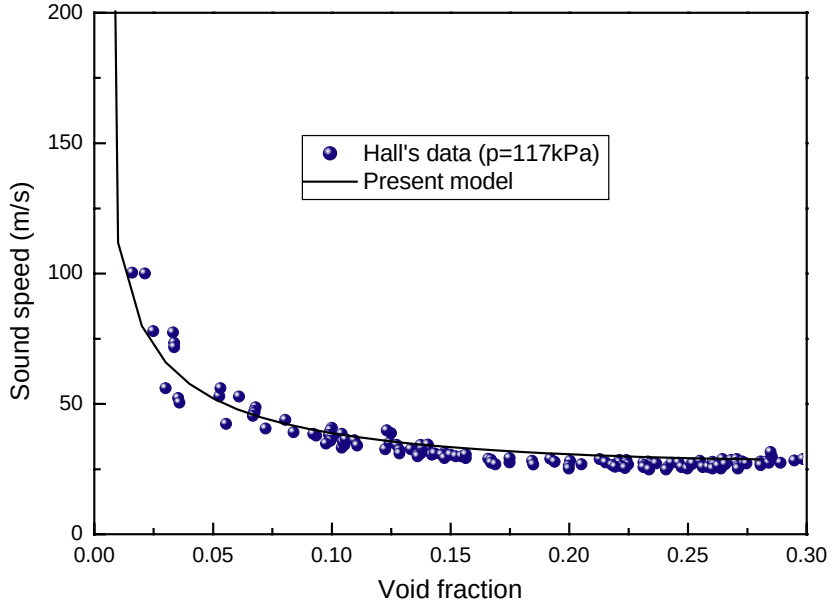

Fig. 3. Sound speed for air/water bubbly flow at $p = 117$ kPa.

difference momentum equation derived from the liquid and vapor momentum equations

$$\frac{\alpha_g \rho_g v_g + \alpha_l \rho_l v_l}{\alpha_g \rho_g + \alpha_l \rho_l} = C_t. \tag{12}$$

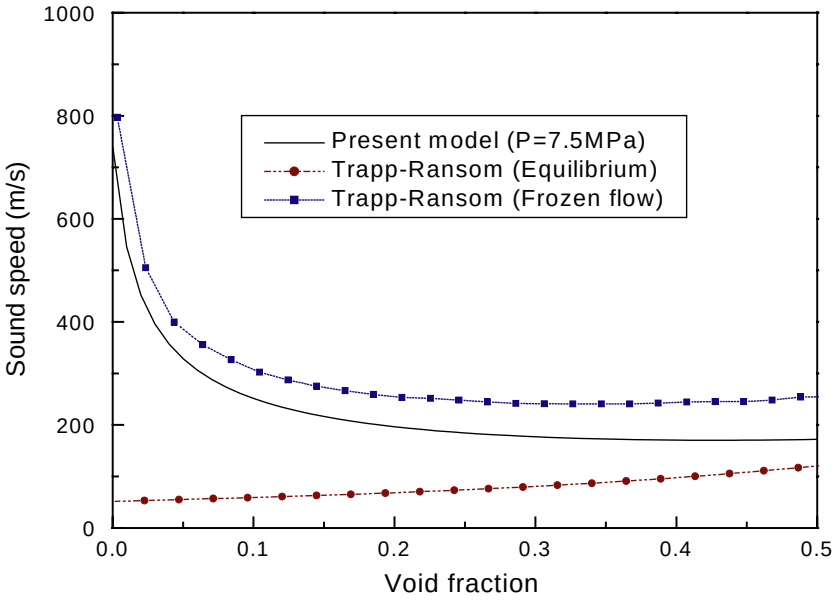

Fig. 4. Comparison of the sound speed derived from the present model with that from the Trapp–Ransom's model at $p = 7.5$ MPa.

It should be noted that the main difference between the Trapp and Ransom's choking criterion [3] and the present one is the definition of total sound speed C_t: We do not use C_t as the sound speed assuming homogeneous equilibrium condition anymore.

It has been known that the Trapp–Ransom's model under the homogeneous equilibrium condition under-predicts the critical flow rates in the bubbly flow regime, $\alpha_g < 0.5$. Because the Trapp–Ransom's model under-predicts the mixture sound speed as shown in Fig. 4, the flow is choked earlier with small discharge rate than that shown in the experimental data.

Because a feature of the equilibrium model is the discontinuity in fluid properties that occurs at the saturation line, there is a discontinuous variation of the sound speed at the transition point from the single-phase water to two-phase mixture using the Trapp–Ransom's model. However, the earlier experimental data for various conditions do not show such a non-physical discontinuity as evidently shown in Figs. 1–3.

On the other hand, the Trapp–Ransom's model derived from the frozen flow assumption excluding phase change over-predicts the sound speed in the bubbly flow regime so that the critical flow rate can be over-estimated. The sound speed criteria under the equilibrium and the frozen flow assumptions show good thermodynamic boundaries of the lower and the upper limitation in the two-phase flow, respectively. Therefore, it is reasonable that the sound speed of non-equilibrium two-phase flow be evaluated between these boundaries as shown in Fig. 4.

In the critical flow model of the MARS code, choking is assumed to occur at the smallest section of the flow fields called throat. The choking criterion can be written in the following form derived by Eq. (10), which is similar to the single phase choking flow criterion and choking corresponding to a total Mach number of unity:

$$M_t \equiv v_t / C_t = \pm 1, \tag{13}$$

where $v_t \equiv (\alpha_g \rho_g v_g + \alpha_l \rho_l v_l)/(\alpha_g \rho_g + \alpha_l \rho_l)$ is the total mixture velocity. In the choking test, the fluid velocity is compared with the local sound speed, which is based on the hydrodynamic conditions at the throat. It is noted that we only apply Eq. (13) with (10) for the calculation of Marviken tests in the initial bubbly flow regime.

If the choking occurs, Eq. (13) is solved semi-implicitly with the upstream vapor and liquid momentum equations for v_g, v_l, and p_g at the point of flow choking [4]. Because the virtual mass terms have a significant effect on the wave propagation [10], we only include such time derivative terms as momentum sources.

5. Marviken tests

In order to validate the present choking criterion, ten Marviken tests [13] are assessed using the MARS code. Among them, three representative results of Marviken test 24 (nozzle length-to-diameter ratio $l/d = 0.3$), test 6 ($l/d = 1.0$), and test 15 ($l/d = 3.6$) with a fixed 30 K subcooling are shown in Figs. 5–7. And the results are compared with the experimental data as well as the earlier calculations by Trapp–Ransom model [3,4]. It should be noted here that we set a discharge coefficient of 1.0 for all discharge periods for assessment and comparison of models though many researchers have generally adopted the discharge coefficients empirically ranged.

The Marviken tests [13] represent large-scale critical flow tests. The pressurized vertical vessel with the total volume of 420 m^3 inserted downward nozzles of various length-to-diameter ratio *l*/*d*, was initially filled with subcooled water and it was used to provide data for the choked discharge flow rate of subcooled water, low quality two-phase mixtures, and steam. The vessel inner-diameter and height are 5.22 and 24.55 m, respectively.

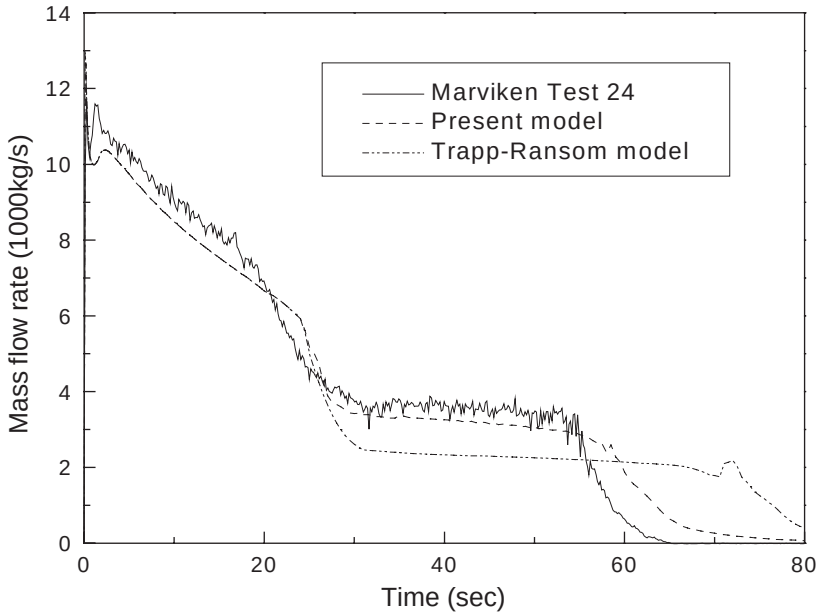

Fig. 5. Comparison between model predictions and measured data for Marviken test 24 (*l*/*d* = 0.3).

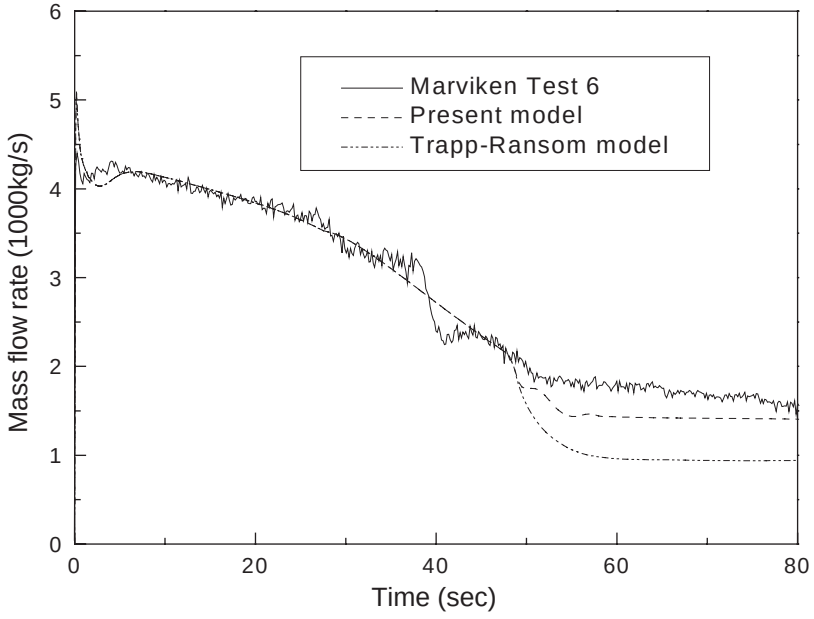

Fig. 6. Comparison between model predictions and measured data for Marviken test 6 ($l/d = 1.0$).

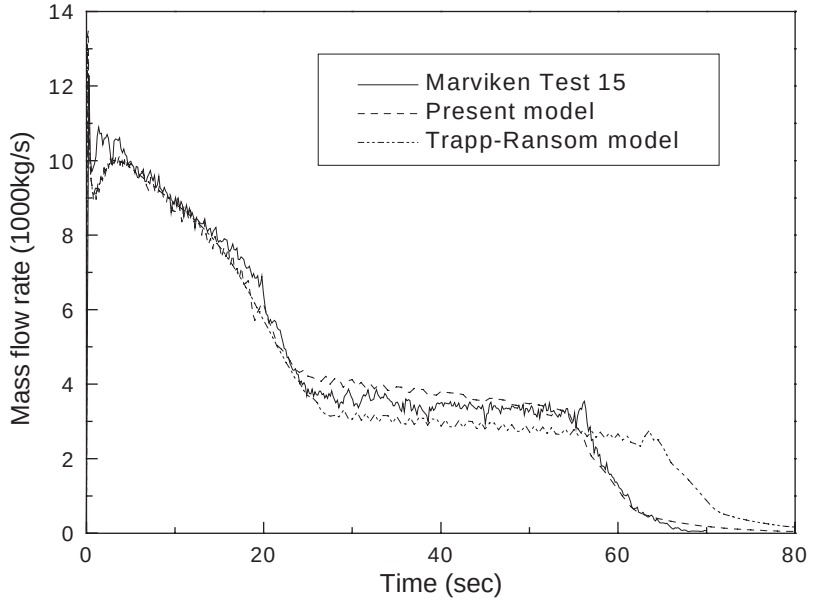

Fig. 7. Comparison between model predictions and measured data for Marviken test 15 ($l/d = 3.6$).

Tests were initiated by failing rupture disks attached to the downstream end of the nozzles and then the subcooled water discharges from the nozzles. The water level in the pressurized vessel was initially at 19.88, 17.81, and 19.93 m for tests 24, 6, and 15, respectively, above the bottom of

vessel, and the steam dome above water levels was saturated at 4.96 MPa for tests 24, 6 and 5.04 MPa for test 15.

During the tests, the subcooling at the nozzle inlet decreased from 60 to 35 K in the first 0.5 s and then decreased gradually until saturated conditions were established at 25 s in tests 25 and 15, and at 50 s in test 6. Two-phase flow period persisted between 25 and 55 s in tests 24 and 15, and after 50 s in test 6. Test data were determined from both pitot-static measurements at the discharge pipe. The transitions from subcooled to saturated bubbly flow are clearly shown in Figs. 5–7. Following discharges of subcooled water, two-phase bubbly flow period is characterized by a steadily decreasing flow rate and pressure.

Figs. 5–7 show the numerical results of the present model at the discharge pipe above the test nozzles in comparison with the experimental data and those of Trapp–Ransom model [3]. In the numerical calculations during the subcooled water discharge using the present model and the Trapp–Ransom model, one single-phase critical flow model is equally used. For this reason, both of the numerical results have the same discharge flow rates until the flow transition from the subcooled water to two-phase bubbly flow.

Although the numerical results do not agree exactly with the experimental data during the subcooled water flow rate, the two-phase critical flow rates calculated using the present model show relatively good agreements with the experimental data as shown in Figs. 5 and 7, whereas those using the Trapp–Ransom model predict critical flow rates much smaller than the experimental data.

On the other hand, the numerical results agree well with the experimental data during the subcooled water discharge, but not during the two-phase bubbly flow discharge in Fig. 6. In spite of discrepancies, the two-phase critical flow rates calculated using the present model still show relatively good results compared with those using the Trapp–Ransom model as shown in Fig. 6.

Consequently, the under-prediction of the Trapp–Ransom model is evident for smaller l/d ratio in which thermal non-equilibrium effect dominates. The present model also reproduces the onset of transition to single-phase vapor discharge in good agreement with experimental data, whereas the transition is prolonged a lot by the Trapp–Ransom model. Although many researchers have generally used the discharge coefficients empirically ranged about 0.8–1.3 to adjust their numerical result to the experimental data, we do not use such adjustments in treating these Marviken test problems.

As shown in Fig. 8, the bubbly flow and the annular flow are dominant flow regimes until the end of the Marviken test procedures at the nozzle outlets. Flow regimes are indicated by the flow regime number, namely, # 4, # 6, and # 7: Number 4, 6, and 7 on the vertical axis represent bubbly, annular, and dispersed flows, respectively. The flow regime transitions from bubbly to annular flow occur abruptly at time 55 and 60 s in the typical test 15 and 24, respectively. Because of the time limits in the real tests, the other transition of flow regimes, from annular flow to dispersed flow, does not exist as shown in Figs. 5 and 7. It should be noticed that these transitions of flow regimes are occurred near the critical point: the critical flow generally occurs at the outlet of the test nozzles below the discharge pipe.

From the assessment results, it is concluded that the present model improves not only the accuracy of the two-phase flow rate but also the transition point from two-phase mixture to single-phase vapor discharge even without the adjustment of discharge coefficient. Thus, MARS code uncertainty related with the critical flow is reduced, which will enhance the code

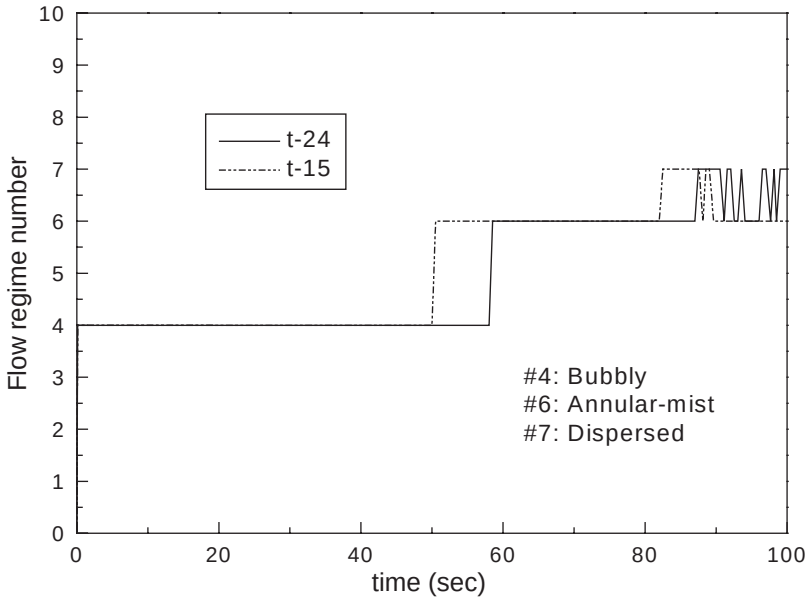

Fig. 8. Flow regime transitions at the nozzle during the Marviken tests 15 and 24.

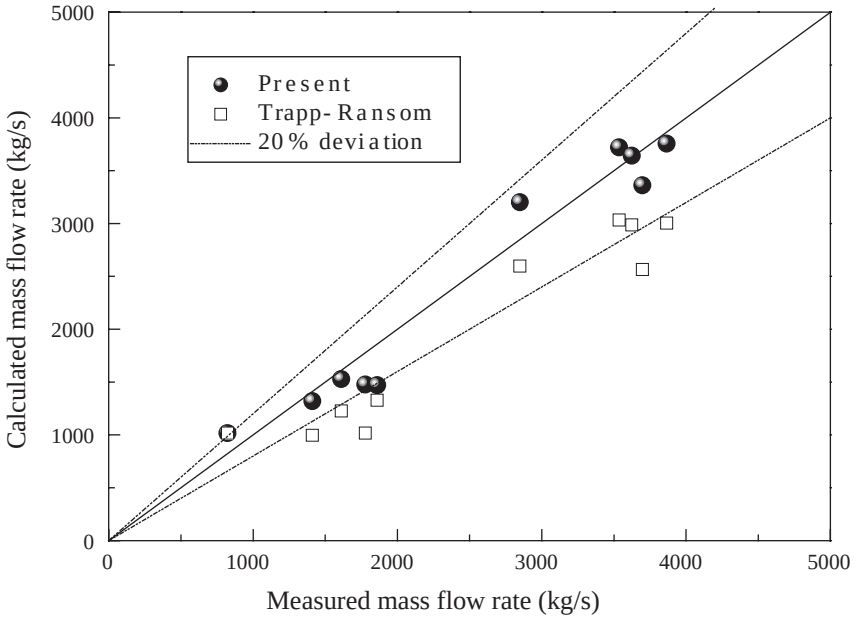

Fig. 9. Calculated mass flow rates vs. experimental data in the bubbly flow regime.

predictability for transient analysis of a thermal hydraulic system. Such improvement mainly owes to the new choking criterion for non-homogeneous and non-equilibrium flow.

As compared in Fig. 9, the present model gives better results than the Trapp–Ransom model does during the two-phase bubbly flow discharges of 10 tests in the various conditions as shown in Table 3.

Table 3
Main characteristics of the Marviken tests

Test number	D (mm)	L (mm)	L/D	Subcooling (°C)	P_{steam} (MPa)	Water level (m)
14	200	590	3.0	30	4.97	18.10
6	300	290	1.0	30	4.95	17.81
26	300	511	1.7	30	4.91	19.31
1	300	895	3.0	15	4.94	19.73
17	300	1116	3.7	30	4.94	19.85
24	500	166	0.3	30	4.96	19.88
21	500	730	1.5	30	4.94	19.95
15	500	1809	3.6	30	5.04	19.93
4	509	1589	3.1	30	4.94	17.59
11	509	1589	3.1	30	4.97	17.63

The mass flow rate obtained by the Trapp–Ransom model is under-predicted with discrepancies of maximum 41% for tests. The relative errors given by the results calculated by the present model during the bubbly flow regime are much smaller than those by the Trapp–Ransom model.

6. Concluding remarks

A new choking criterion for two-phase bubbly flow has been developed based on the hyperbolic two-fluid model for non-equilibrium and non-homogeneous flow. The hyperbolic two-fluid model employs the interfacial pressure jump terms in momentum equations derived from the concept of surface tension. Total sound speed of two-phase mixture is analytically derived from the system eigenvalues obtained using the characteristic analysis of the hyperbolic two-fluid model. It is found that this analytic sound speed agrees well with the earlier experimental data and shows better prediction in some cases compared with the previous models of Nguyen and Trapp–Ransom. This new choking criterion has been implemented in the MARS code and assessed by Marviken critical flow tests. From the assessments, it is validated that the new choking criterion improves not only the accuracy of two-phase critical flow rate but also the transition point even without any adjustment using discharge coefficients. In conclusion, this choking criterion improves the accuracy of two-phase critical flow, thus, enhances the MARS code capability for the realistic simulation of thermal hydraulic system transients.

Acknowledgements

The authors gratefully acknowledge the valuable discussion with Dr. Won-Jae Lee and Dr. Bub-Dong Chung.

References

[1] F.J. Moody, Maximum flow rate of a single-component, two-phase mixture, *Transactions of American Society of Mechanical Engineers, Journal of Heat Transfer* 87 (1965) 134–142.

[2] R.E. Henry, H.K. Fauske, The two-phase critical flow of one-component mixtures in nozzles orifices and short tube, *Transactions of American Society of Mechanical Engineers, Journal of Heat Transfer* 93 (1971) 179–187.
[3] J.A. Trapp, V.H. Ransom, Choked flow calculation criterion for nonhomogeneous nonequilbrium two-phase flows, *International Journal of Multiphase Flow* 8 (1982) 669–681.
[4] J.-J. Jeong, K.S. Ha, B.D. Chung, W.J. Lee, Development of a multi-dimensional thermal hydraulic system code, MARS 1.3.1, *Annals of Nuclear Energy* 26 (1999) 1611–1642.
[5] D.A. Drew, L.Y. Cheng, R.T. Lahey Jr., The analysis of virtual mass effects in two-phase flow, *International Journal of Multiphase Flow* 5 (1979) 233–242.
[6] A.R.D. Thorley, D.C. Wiggert, The effect of virtual mass on the basic equations for unsteady one-dimensional heterogeneous flows, *International Journal of Multiphase Flow* 12 (1985) 149–160.
[7] H.B. Stewart, Stability of two-phase flow calculation using two-fluid models, *Journal of Computational Physics* 33 (1979) 259–270.
[8] S.J. Lee, K.S. Chang, S.J. Kim, Surface tension effect in the two-fluid equation system, *International Journal of Heat and Mass Transfer* 41 (1998) 2821–2826.
[9] M.S. Chung, K.S. Chang, S.J. Lee, Numerical solution of hyperbolic two-fluid two-phase flow model with non-reflecting boundary conditions, *International Journal of Engineering Science* 40 (2002) 789–803.
[10] M.S. Chung, S.J. Lee, K.S. Chang, Effect of interfacial pressure jump and virtual mass terms on sound wave propagation in the two-phase flow, *Journal of Sound and Vibration* 244 (2001) 717–728.
[11] M.S. Chung, S.J. Lee, W.J. Lee, K.S. Chang, An interfacial pressure jump model for two-phase bubbly flow, *Numerical Heat Transfer-Part B* 40 (2001) 83–97.
[12] K.L. Nguyen, E.R.F. Winter, M. Greiner, Sonic velocity in two-phase systems, *International Journal of Multiphase Flow* 7 (1981) 311–320.
[13] The Marviken Full-Scale Critical-Flow Tests, NUREG/CR-2671, MXC-301, 1982.
[14] M. Ishii, K. Mishima, Study of two-fluid model and interfacial area, NUREG/CR-1873, ANL-80-111, Argonne National Laboratory, 1980.
[15] G.B. Whitham, *Linear and Nonlinear Waves*, Wiley, New York, 1974.
[16] R.E. Henry, M.A. Grolmes, H.K. Fauske, Pressure pulse propagation in two-phase one- and two-component mixtures, ANL-7792, 1971.
[17] H.B. Karplus, Propagation of a pressure wave in a mixture of water and steam, Armour Research Foundation of Illinois Institute of Technology Report 4132, 1961.
[18] V.E. Nakoryakov, The wave dynamics of vapor–liquid medium, *International Journal of Multiphase Flow* 14 (1988) 655–677.
[19] D.G. Hall, An inventory of the two-phase critical flow experimental data base, EGG-CAAP-5140, June 1982.
[20] A.E. Ruggles, The Propagation of Pressure Perturbations in Bubbly Air/Water Flow, PhD Thesis (Nuclear engineering), Rensselaer Polytechnic Institute, 1987.